Journal of Thermal Analysis and Calorimetry, Vol. 73 (2003) 745–753

CRYSTALLIZATION KINETICS OF AMORPHOUS $Fe_{75-x}Cu_xSi_9B_{16}$

K. Chrissafis[*]

Physics Department, Aristotle University of Thessaloniki, GR 54124 Thessaloniki, Greece

(Received November 15, 2002; in revised form March 11, 2003)

Abstract

In this work the influence of Cu admixtures on the crystallization process of amorphous Fe–Si–B alloys is studied, based on measurements of differential thermal calorimetry of the series $Fe_{75-x}Cu_xSi_9B_{16}$ (x=0, 1, 2, 2.8 and 3.5) during their heating with different heating rates. The first crystallization stage can not be traced for any of the amounts of Cu content examined, while the second stage is observed only when the Cu content is 1 at%. The activation energy as estimated with Kissinger's method for the third crystallization stage has a mean value of 326 kJ mol^{-1} and with the isoconversional Flynn, Wall and Ozawa method is almost constant when $0.05<\alpha<0.6$ and exhibits a small monotical decrease when $\alpha>0.6$. The main crystallization peak can not be described by means of a single JMA-type function.

Keywords: activation energy, crystallization, DSC, Fe–Si–B

Introduction

Many studies have been carried out during the last decade, aiming at the amelioration of the soft magnetic properties of the amorphous Fe–Si–B alloys. The tools used towards this aim are mainly the thermal treatment of the said alloys and their enrichment with various admixtures. A typical example is the preparation of nanocrystalline materials with stoichiometry $Fe_{74}Cu_1Nb_3Si_9B_{13}$ [1], having much better soft magnetic properties than the corresponding ones of the amorphous materials.

This work focuses on the influence of Cu admixtures on the kinematics of the crystallization of the amorphous Fe–Cu–Si–B alloys. In our previous works [2, 3], based on measurements of the saturation magnetization, electrical resistance and electron microscopy (TEM) of the alloy series $Fe_{75-x}Cu_xSi_9B_{16}$ (x=0, 1, 2, 2.8 and 3.5) and on the work of other researchers as regards the crystallization of Fe–Si–B alloys, the following conclusions were arrived at:

The crystallization of the amorphous alloys $Fe_{75-x}Cu_xSi_9B_{16}$ is completed in three stages, corresponding to the growth of bcc Fe[Si,Cu], then of bct Fe_3B and finally to the disintegration of the latter into bcc Fe and bct Fe_2B. The final product of the crystallization consists of 52% $Fe_{83-c}Cu_cSi_{17}$ ($c=x/0.52$) and 48% Fe_2B.The presence of Cu admix-

* Author for correspondence: E-mail: hrisafis@physics.auth.gr

1388–6150/2003/ $ 20.00
© 2003 Akadémiai Kiadó, Budapest
Akadémiai Kiadó, Budapest
Kluwer Academic Publishers, Dordrecht

tures in the amorphous material causes microsegregation, leading to an increase of the crystallization rate. As the ratio of the number of B atoms to the number of Fe atoms increases, the crystallization of bct Fe_3B is favored and that of bcc Fe is hindered.

The aim of the present work is to validate and supplement the above conclusions by measurements of differential scanning calorimetry (DSC), so that a more complete picture of the crystallization procedure of the alloys under investigation can be drawn.

Experimental procedure

Four amorphous ribbons with stoichiometry $Fe_{75-x}Cu_xSi_9B_{16}$ (x=0, 1, 2, 2.8 and 3.5) were prepared in a melt-spinning machine (single-roll quenching technique), the alloys having been prepared in an arc-melting apparatus, from 3N+ purity elements. The composition of the alloys was verified, as regards the relative ratios of Fe, Cu and Si, by SEM. Regarding B, its atomic percentage was set from the mass of B added to form the alloy.

The thermal behaviour of $Fe_{75-x}Cu_xSi_9B_{16}$ was studied using Setaram DSC-131. Temperature and energy calibrations of the instrument were performed using the well-known melting temperatures and melting enthalpies of high purity zinc and indium supplied with the instrument. Ribbon-shaped specimens weighing about 7 mg, cut into small pieces were crimped in stainless steel crucibles, an empty stainless steel crucible was used as reference. A constant flow of nitrogen was maintained in order to provide a constant thermal blanket within the DSC cell, thus eliminating thermal gradients, and ensuring the validity of the applied calibration standard from sample to sample.

A series of non-isothermal DSC experiments was carried out on the $Fe_{75-x}Cu_xSi_9B_{16}$ ribbons with heating rates in the range 3–12.5 K min^{-1}.

Results and discussion

Figure 1 shows, for example, the DSC curves of the rapidly quenched $Fe_{75-x}Cu_xSi_9B_{16}$ alloys containing 0, 1 and 2 at% Cu obtained with a heating rate of 3 K min^{-1}. None of the observed anomalies was reproduced in the subsequent measuring run on the crystallized samples. In comparing these figures, we notice that there is a distinct difference in the

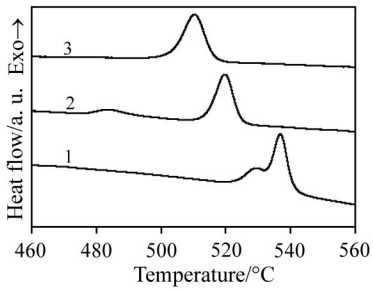

Fig. 1 DSC linear heating curves of $Fe_{75-x}Cu_xSi_9B_{16}$ with heating rate 3 K min^{-1}
1 – 0 at% Cu, 2 – 1 at% Cu, 3 – 2 at% Cu

peak morphology of the DSC curves. We observe that the addition of Cu by replacing Fe results to the appearance of two distinct peaks when the concentration of Cu is 1 at%. Further increase in the Cu content leads to the first peak not being observed.

The difference between the glass-like and crystal-like specific heats of $Fe_{75-x}Cu_xSi_9B_{16}$ is small relatively to the heights of the crystallization apparent specific heat peaks. The dependence of the degree of transformation α on temperature is calculated for different heating rates. The fraction transformed, α, is obtained from the DSC curves as follows: $\alpha(T,t)=\Delta H(T,t)/\Delta H_{cryst}$ where ΔH_{cryst} and $\Delta H(T,t)$ are the total and partial transformation enthalpies.

Figure 2 shows the DSC curves of $Fe_{75-x}Cu_xSi_9B_{16}$ alloys containing 0, 1, 2, 2.8 and 3.5 at% Cu obtained with a heating rate of 3 K min^{-1} after the subtraction of the base line. For the material without Cu, the crystallization procedure evolves through a temperature range of 30°C. The admixture of Cu widens this range for the concentration 1 at% Cu and shifts the phenomenon towards lower temperatures for all the concentrations. The increase in the Cu content above 2 at% (samples 4, 5) leads to a shift of the peak maximum towards higher temperatures which, however, are lower than the peak maximum temperature of the sample without Cu. In the temperature range from 400–500°C no exothermic peak appears when the concentration is from 2–3.5 at% Cu, as mentioned above.

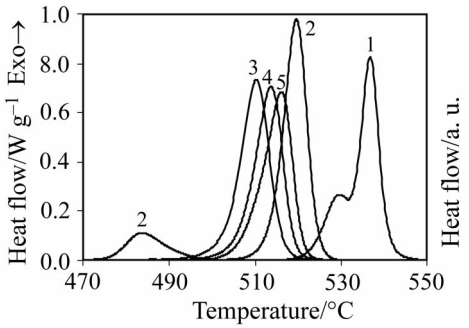

Fig. 2 DSC linear heating curves of $Fe_{75-x}Cu_xSi_9B_{16}$ with heating rate 3 K min^{-1} after the subtraction of the base line. 1 – 0 at% Cu, 2 – 1 at% Cu, 3 – 2 at% Cu, 4 – 2.8 at% Cu, 5 – 3.5 at% Cu

From previous works it is known that the crystallization is completed in three stages. From the fact that the first stage (300–400°C) is not observed in the measurements of the saturation magnetization [2] and from the overall decrease of the electrical resistance [3], the conclusion is drawn that the first stage gradually disappears as the Cu concentration increases. For this reason this effect is not evidenced by the thermal measurements. As noticed by TEM observations [3], at these temperatures dendrites of bcc Fe[Si,Cu] start to grow.

At 450°C the second stage starts, where eutectic bcc Fe[Si,Cu]+bct Fe_3B is formed. A characteristic of this crystallization is that it takes place mainly among the dendrites and only sparsely in the form of isolated spherulites. The growth depends on both the size and the number of the bcc Fe[Si,Cu] crystallites. This is probably the main reason why, although the quantity of the material crystallized during the first

stage decreases with increasing concentration of admixtures, the second stage is accelerated and effected at lower temperatures.

The volume of the material crystallized during the second stage is greater than that of the first, but there still remains a high amount of amorphous material among the already crystalline regions. The crystallization is integrated at a third stage, by 500°C, when the metastable bct Fe_3B compound is first formed and then separated into bcc Fe and bct Fe_2B. As a result, the volume occupied by the amorphous material is now filled with grains presenting a lamellar microstructure. This striped contrast is most probably due to much more complicated multiphase microstructure than the successive layers of the two simple bcc Fe and bct Fe_2B phases, as these also include their stoichiometric fluctuations.

For the alloys with more than 1 at% Cu, the final product of the crystallization consists of the smallest and most well-formed regions. This is due to the fact that, during the first two stages, both the crystalline and the remaining amorphous material are confined in regions with areas that get smaller as the Cu concentration increases. Now, it is evident that the less the area of the remaining amorphous regions, the swifter the completion of the third stage.

These conclusions are in absolute accordance with the experimental results of DSC measurements.

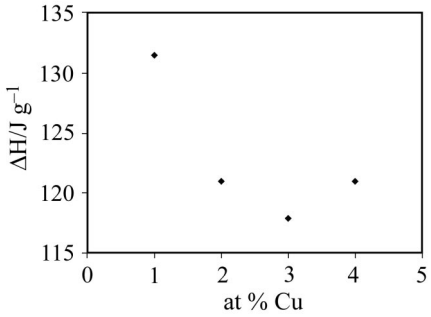

Fig. 3 Compositional dependence of the enthalpy (ΔH)

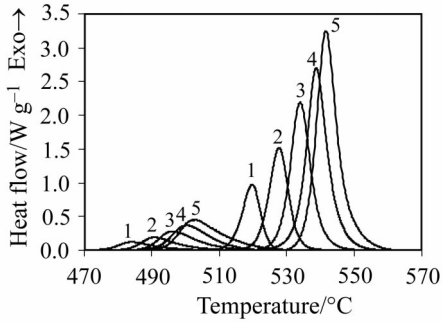

Fig. 4 Non-isothermal DSC crystallization curves of 1 at% Cu with two exothermic peaks under different heating rates (β K min^{-1}). 1 – β=3, 2 – β=5, 3 – β=7.5, 4 – β=10, 5 – β=12.5

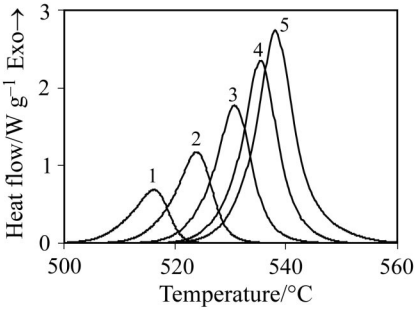

Fig. 5 Non-isothermal DSC crystallization curves of 4 at% Cu with one exothermic peak under different heating rates (β K min^{-1}). 1 – β=3, 2 – β=5, 3 – β=7.5, 4 – β=10, 5 – β=12.5

Figure 3 shows the compositional dependence of the ΔH values evaluated from the previously mentioned DSC curves only for the main curve. It is seen in the former that the enthalpy tends to gradually decrease with increasing Cu content up to 2.8 at%, and then it slightly increases through the further addition of Cu.

A series of DSC experiments was carried out with continuous heating rates in the range 3–12.5 K min^{-1}, as shown in Figs 4 and 5 for two of the compositions 1 and 3.5 at% Cu. It is clear that the peak temperature, T_p, shifts higher with increasing heating rate, while at the same time the peak height increases and the area under the crystallization exotherm also increases.

Kinetic analysis

For the study of crystallization kinetics we assume that each crystallization peak can be described by a kinetic equation of the form

$$d\alpha/dt=k(T)f(\alpha) \quad (1)$$

where

$$k(T)=A\exp[-E/(R/T)] \quad (2)$$

is the Arrhenius temperature – dependent rate constant, E is the activation energy, A is the pre-exponential factor and $f(\alpha)$ characterizes the type of transformation mechanism.

On the basis of the dynamic DSC measurements at various heating rates the isoconversional method [4, 5] of Flynn, Wall and Ozawa [6] was used. This is a model free method which involves measuring the temperatures corresponding to fixed values of α from experiments at different heating rates, β, and plotting ln(β) *vs*. $1/T$

$$\ln(\beta) =\ln[Af(\alpha)d\alpha/dT] - E/RT \quad (3)$$

and the slopes of such plots give $-E/R$.

If the determined activation energy is the same for the various values of α, the existence of a single-step reaction can be concluded with certainty. On the contrary, a

change of E with increasing degree of conversion is an indication of a complex reaction mechanism that invalidates the separation of variables involved in the OFW

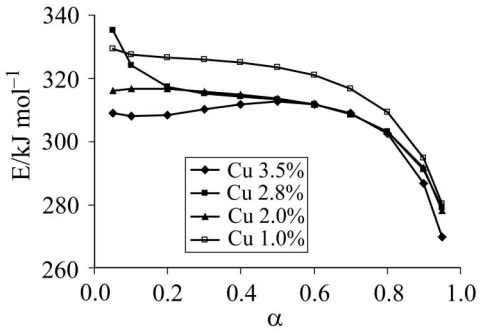

Fig. 6 The dependence of the activation energy calculated by the isoconversional method of Ozawa on the degree of conversion

analysis [7]. These complications are especially serious if the total reaction involves competitive reaction mechanisms.

Figure 6 shows the variation of E with α, for the main peak for all the compositions. We notice that E is approximately the same for all the stoichiometries, it is constant for the range $0.1<\alpha<0.6$, whereas for values larger than 0.6 a small decrease in the value of E is observed. This kind of dependence results to the conclusion that we probably do not have a single-step reaction and this is an indication of a complex reaction mechanism.

The activation energy of crystallization (E) was estimated also using the Kissinger's method [8] which relates the dependence of T_p on β (heating rate) by the following equation

$$\ln(\beta/T_p^2) = -E/RT_p + \ln(AR/E) \quad (4)$$

The value of E (kJ mol^{-1}) was obtained from the slope of $\ln(\beta/T_p^2)$ *vs.* $1000/T_p$ plot given in Fig. 7 and also the pre-exponential factor A (s^{-1}) from the intercept.

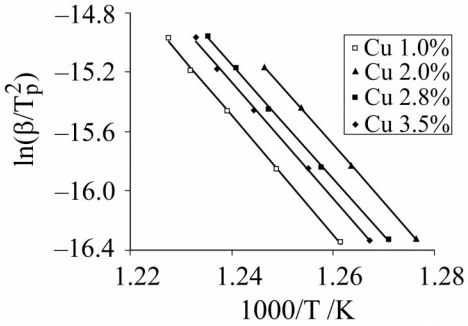

Fig. 7 The Kissinger plots of the heating rate shift in the DSC peak temperature

From this we can calculate the main value of the rate constant for the peak temperature. Table 1 shows the values of the activation energy, the pre-exponential factor and the rate constant for all the concentrations of Cu. We notice that the values of the activation energy as they are calculated with the Kissinger's method are a little larger than the corresponding ones calculated with the method of Flynn, Wall and Ozawa for the peak temperature.

Table 1 Activation energy, pre-exponential factor and mean value of the rate constant for different concentration of Cu

at% Cu	E/kJ mol^{-1}	A/s^{-1}	$k(T)$/s^{-1}
1	336.9	$2.81\cdot10^{19}$	$4.38\cdot10^{-3}$
2	321.4	$8.48\cdot10^{18}$	$7.61\cdot10^{-3}$
2.8	319.4	$4.96\cdot10^{18}$	$7.68\cdot10^{-3}$
3.5	327.1	$1.41\cdot10^{19}$	$7.71\cdot10^{-3}$

The crystallization kinetics is usually interpreted in terms of the standard nucleation-growth model formulated by Johnson–Mehl–Avrami (JMA) [9, 10]. This model describes the time dependence of the fractional crystallization α, usually written in the following form

$$\alpha=1-\exp[-(kt)^n] \tag{5}$$

where the rate constant k is a function of temperature and in general depends on both the nucleation frequency and the crystal growth rate, and the kinetic exponent n is a parameter which reflects the nucleation frequency and/or the growth morphology [10]. The rate equation can be obtained from Eq. (5) by differentiation with respect to time:

$$(d\alpha/dt)=kn(1-\alpha)[-\ln(1-\alpha)]^{1-1/n} \tag{6}$$

Equation (6) is usually referred to as the JMA equation, and it is frequently used for the formal description of TA crystallization data. It should be emphasized, however, that validity of the JMA equation is based on the following assumptions [11, 12]: (a) Isothermal crystallization conditions, (b) Low anisotropy of growing crystals, (c) Homogeneous nucleation or heterogeneous nucleation at randomly dispersed second-phase particles, and (d) Growth rate of new phase controlled by temperature and independent of time.

Henderson [11, 12] has shown that the validity of the JMA equation can be extended in non-isothermal conditions if the entire nucleation process takes place during the early stages of the transformation, and it becomes negligible afterward. The crystallization rate is controlled only by temperature and does not depend on the previous thermal history. Although the limits of applicability of the JMA equation are well known, in practice it is not so easy to verify whether the conditions of applicability are fulfilled or not.

One of the testing method for non-isothermal data is an inspection of the linearity of the Avrami (JMA) plot. Matusita *et al*. [13, 14] extending the use of the JMA

equation, have suggested an equation which is applicable for non-isothermal crystallization and is given by

$$\ln[-\ln(1-\alpha)] = -n\ln(\beta) - 1.052\, mE/RT + \text{const.} \quad (7)$$

where α is the volume of the fraction crystallized at any temperature, m and n are numerical factors depending on the nucleation process and growth morphology.

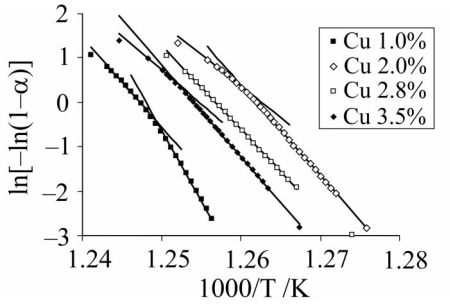

Fig. 8 Avrami plots of $\ln[-\ln(1-\alpha)]$ as a function of reciprocal temperature $1000/T$

When nuclei (formed during the heating at constant rate) are dominant, n is equal to (m+1) and when nuclei (formed in the previous heating treatment before the thermal analysis run) are dominant, n is equal to m. Also, m=3 for three- dimensional growth of crystal particles, m=2 for two-dimensional growth and m=1 for one dimensional growth. The plot of $\ln[-\ln(1-\alpha)]$ as a function of reciprocal temperature $1/T$ should be linear. Nevertheless, it is well known that a double logarithmic function, in general, is not very sensitive to subtle changes to its argument. Therefore, one can expect that the plots of $\ln[-\ln(1-\alpha)]$ *vs*. $1/T$ may be linear even in the case that the JMA model is not fulfilled.

The plot of $\ln[-\ln(1-\alpha)]$ as a function of reciprocal temperature $1/T$ is shown in Fig. 8 for all the concentrations and heating rate equal to 5 K min^{-1}. We notice the appearance of two regions with a different slope. This difference is generally small, it vanishes when the Cu concentration is 2.8 at% and it slightly increases when the Cu concentration is 1 at%. The slope of the lines in the region $0.1<\alpha<0.8$ with 2, 2.8, and 3.5 at% Cu, in the region $0.5<\alpha<0.9$ for the main peak and in the region $0.1<\alpha<0.4$ for the first peak appearing when the Cu content is 1 at%, is about the same. The main difference in the slopes appears with 1 at% Cu in the regions $0.4<\alpha<0.8$ and $0.1<\alpha<0.5$ for the first and the main peak correspondingly. For the calculation of m we use the value of the activation energy that we have estimated with the Kissinger method. With the help of least squares fitting we calculate m ($=4.7\pm0.2$) from their slope. The calculated value of m is larger than the theoretically anticipated with the JMA model, although the requirement of line formation is satisfied for a wide range of values of α. The slope difference, which is significant with 1 at% Cu and the variation of the m value from the theoretically estimated ones indicate increasing complexity of the process, and probably, there is a low mutual overlapping of the nucleation and growth phases.

Conclusions

The first crystallization stage can not be traced for any of the amounts of Cu content examined, because the fraction of crystallization is very small, while the second stage is observed only when the Cu content is 1 at%. The activation energy as estimated with the Kissinger's method for the third crystallization stage, is about the same for all the four values of Cu concentration and has a mean value of 326 kJ mol^{-1}. The activation energy calculated with the isoconversional Flynn, Wall and Ozawa method is almost constant when $0.05<\alpha<0.6$ and exhibits a small monotical decrease when $\alpha>0.6$. The dependence of $\ln(-\ln(1-\alpha))$ on $1000/T$ exhibits two linear regions with a small slope difference, which increases when the Cu content is 1 at% and the values of m are larger than the theoretically estimated. The results of the Electronic Microscopy analysis, the dependence of E on α and the appearance of two linear regions in the Avrami plot, indicate that in the crystallization peak corresponding to the third stage different nucleation and growth mechanisms may simultaneously happen, thus making impossible the description of $f(\alpha)$ by means of a single JMA-type function.

References

1 Y. Yoshizawa, S. Oguma and K. Yamauchi, J. Appl. Phys., 64 (1988) 6044.
2 K. G. Efthimiadis, C. A. Achilleos, S. C. Chadjivasiliou and I. A. Tsoukalas, J. Magn. Magn. Mat., 171 (1997) 141.
3 K. G. Efthimiadis, E. K. Polychroniadis, S. C. Chadjivasiliou and I. A. Tsoukalas, Mat. Res. Bul., 35 (2000) 937.
4 S. Vyazovkin, J. Therm. Anal. Cal., 64 (2001) 829.
5 P. Budrugeac, D. Homentcovschi and E. Segal, J. Therm. Anal. Cal., 63 (2001) 457.
6 T. Ozawa, J. Thermal Anal., 2 (1970) 301.
7 T. Ozawa, Bull. Chem. Soc. Japan, 38 (1965) 1881.
8 H. E. Kissinger, J. Res. Nat. Bur. Stan., 57 (1956) 217.
9 M. Avrami, J. Chem. Phys., 9 (1941) 177.
10 W. A. Johnson and R. F. Mehl, Trans. Am. Inst. Min. (Metal.) Eng., 135 (1939) 416.
11 D. W. Henderson, J. Thermal Anal., 15 (1979) 325.
12 D. W. Henderson, J. Non-Cryst. Solids, 171 (1994) 141.
13 K. Matusita, T. Konatsu and R. Yokota, J. Mater. Sci., 19 (1984) 291.
14 K. Matusita and S. Sakka, Phys. Chem. Glasses, 20 (1979) 81.